Advances in Nano Research, *Vol. 16, No. 1 (2024) 27-40*
https://doi.org/10.12989/anr.2024.16.1.027

Nonlocal Mindlin plate theory with the application for vibration and bending analysis of nanoplates with the flexoelectricity effect

Pham Ba Khien[1], Du Dinh Nguyen[2] Abdelouahed Tounsi[3,4,5,6] and Bui Van Tuyen*[7]

[1]*HUTECH institute of Engineering, HUTECH University, Ho Chi Minh, Vietnam*
[2]*Faculty of Civil Engineering, Lac Hong University, Dong Nai Province, Viet Nam*
[3]*Department of Civil and Environmental Engineering, King Fahd University of Petroleum & Minerals, 31261 Dhahran, Eastern Province, Saudi Arabia*
[4]*Material and Hydrology Laboratory, University of Sidi Bel Abbes, Faculty of Technology, Civil Engineering Department, Algeria*
[5]*Department of Civil and Environmental Engineering, Lebanese American University, 309 Bassil Building, Byblos, Lebanon*
[6]*YFL (Yonsei Frontier Lab), Yonsei University, Seoul, Korea*
[7]*Faculty of Mechanical Engineering, Thuyloi University, 175 Tay Son, Dong Da, Hanoi, Vietnam*

(*Received December 22, 2022, Revised August 17, 2023, Accepted August 28, 2023*)

Abstract. This work is the first of its kind to integrate Mindlin's theory with analytical methods in order to produce an exact solution to a specific vibration issue as well as a bending problem involving a nanoplate that is supported by a viscoelastic foundation. The plate is exposed to the simultaneous effects of a compressive load in the plate plane and a force operating perpendicular to the plane of the nanoplate. In addition, the flexoelecity effect is included into the plate. The strain gradient component is taken into consideration while calculating the plate equilibrium equation using the nonlocal theory and Hamilton's principle. The free vibration and static responses of the nanoplate seem to be both real and imaginary components because of the appearance of the viscoelastic drag coefficient of the viscoelastic foundation. This study also shows that when analyzing the mechanical response for nanostructure, taking into account the flexoelectricity effect and the influence of the nonlocal parameter, the results will be completely different from the case in which this parameter is ignored. This indicates that it is vital to take into consideration the effects of nonlocal parameters on the nanosheet structure while also taking into consideration the effect of flexoelectricity.

Keywords: analytical method; bending; flexoelectricity; free vibration; nanoplates; viscoelastic foundation

1. Introduction

This work is the first of its kind to integrate Mindlin's theory with analytical methods in order to produce an exact solution to a specific vibration issue as well as a bending problem involving a nanoplate that is supported by a viscoelastic foundation. The plate is exposed to the simultaneous effects of a compressive load in the plate plane and a force operating perpendicular to the plane of the nanoplate. In addition, the flexoelecity effect is included into the plate. The strain gradient component is taken into consideration while calculating the plate equilibrium equation using the nonlocal theory and Hamilton's principle. The free vibration and static responses of the nanoplate seem to be both real and imaginary components because of the appearance of the viscoelastic drag coefficient of the viscoelastic foundation. This study also shows that when analyzing the mechanical response for nanostructure, taking into account the flexoelectricity effect and the influence of the nonlocal parameter, the results will be completely different from the case in which this parameter is ignored. This indicates that it is vital to take into consideration the effects of nonlocal parameters on the nanosheet structure while also taking into consideration the effect of flexoelectricity.

Micro- and nano-electro-mechanical systems are mostly driven by the contributions of their intelligent subsystems. In general, the performance of certain tasks requires electromechanical coupling effects, such as piezoelectric effect, which are provided by intelligent components. On the other hand, the fexoelectric effect has been getting a lot of attention as of late. Higher-order electromechanical coupling effects, such as the Flexoelectric effect, have a wide range of applications in a wide range of industries (Shu *et al*. 2019, Zubko *et al*. 2013). This higher-order electromechanical connection is known as the flexoelectric effect. Because it is present in all dielectric materials, the fexoelectric effect opens up a wider range of materials for usage in electromechanical applications. In addition, because it is size dependent, the fexoelectric effect will be amplified at the nanoscale. For electromechanical applications, this allows for a wider range of materials. More materials may be used in electromechanical applications as a result of this.

The mechanical behavior of structures that are impacted by the flexoelectricity effect has been the primary focus of research conducted by scientists as a foundation for the design, production, and use of the micro- and nano-structures. According to Shen and Hu (2010), nano-dielectrics may be coupled to each other through flexo-electricity, surface effect, and electrostatic force. The effect

*Corresponding author, Ph, D.,
E-mail: tuyenbv@tlu.edu.vn

ISSN: 2287-237X (Print), 2287-2388 (Online)

of flexoelectricity on nanoscale piezoelectric beam bending and vibration was studied by Yan and Jiang (2013a, b), Ebrahimi *et al*. (2019a). Bernouli–Euler beam model was utilized by Liang *et al*. (2014, 2015) to investigate the effects of surface and flexoelectricity on piezoelectric nanobeam bending. An investigation of fairly thick beams was conducted by Yue *et al*. (2016) that included evaluation of flexoelectric effects on the surface and the bending and vibration difficulties. The Timoshenko beam theory was used in their therapy. Piezoelectric nanobeams with geometrical imperfections and flexoelectric effects may be simulated using the finite element method (FEM) and an unique third-order shear deformation beam theory. Tho *et al*. (2021) the FEM with a novel third-order shear deformation beam theory (TSDT), in which, the structures are placed on Pasternak's elastic foundations. Deng *et al*. (2014) performed research on the harvesting of flexoelectric energy when it was exposed to harmonic mechanical stimulation for a nanoscale beam. This study was the result of the researchers' efforts. Their research showed that the efficiency of the flexoelectric conversion was enhanced. Following an investigation into the influence of the flexoelectric effect on the buckling and vibration behavior of piezoelectric nanofilms, Liang *et al*. (2016) came to the conclusion that the flexoelectric effect significantly raises both the critical buckling loads and the natural frequencies. This was the conclusion that was reached as a result of the investigation. Qi *et al*. (2016) investigated the static bending of bilayer cantilever beams under closed and open conditions respectively. In a subsequent investigation, Qi *et al*. (2018) colleagues looked into the electromechanical responses of a curved flexoelectric microbeam. By basing their work on the theory of nonlocal elasticity, Rupa and Ray (2017) were able to establish the ideal solution for the static bending of simply supported flexoelectric nanobeams. Using the two-dimensional theory of elasticity, Xiang and Li (2018) were able to provide an accurate solution for the bending of an elastic beam that took into account both the flexoelectric and piezoelectric effects. In their study, Xiang and Li applied the theory of elasticity to two dimensions. Taking into consideration the flexoelectric effect, Xiang *et al*. (2020) extended the previously reported findings to the static bending of a functionally graded beam. This was accomplished by taking into account the flexoelectric effect. Hieu *et al*. (2020) carried out an experimental study to enhance the quality of the characteristic transmittance curve in the infrared range of 2.5-7 μm of the optical magnesium fluoride (MgF2) ceramic. Which is used a lot in power generation equipment. The Kirchhoff thin plate theory (Yang *et al*. 2015), clamped boundary circumstances (Zhang *et al*. 2014), and cantilevered boundary conditions (Wang *et al*. 2017), respectively, have been used in order to examine the flexoelectric influence on the bending behavior of piezoelectric nanoplates. Navier's technique is used to find solutions to the motion equations for nanobeams that are simply supported. Majdoub *et al*. (2008) conducted research on the influence of flexoelectric effects and piezoelectric effects on mechanical behavior. They found that the flexoelectric effect has a notable scale effect, particularly at the nanoscale. Research on the flexoelectric effects of a heterogeneous flexoelectric membrane was carried out by Mohammadi *et al*. (2014), who also projected the effective electromechanical features of the membrane. During the course of their study, Li *et al*. 2016 investigated the fexoelectric responses of a circular plate. Ghobadi *et al*. (2021) looked at the nonlinear behavior of a functionally graded fexoelectric nano-plate in the context of a temperature setting. In addition, the capacity to collect energy of a fexoelectric plate that was attached on an elastic substrate was investigated, and the optimal inner and outer radii for producing the most amount of power were found (Wang and Wang 2018). To investigate the vibration and static bending response of nanoplates, Thai *et al*. (2022), Doan *et al*. (2022) employ the finite element technique. These calculations factor in the influence of flexoelectricity. Phung *et al*. (2022) analyzed the mechanical response of rectangular plates subjected to static loads and supported on a discontinuous two-parameter elastic foundation.

When beams or plates are supported by other objects, depending on the specific foundation theories, they are frequently described as resting on either an elastic foundation (described by springs) or a viscoelastic foundation (through the viscous drag coefficient). In addition, there have been a great number of scientific publications that have focused on analyzing the mechanical behavior of structures that are built on such foundations. Duc *et al*. (2022) uses the finite element method to simulate the specific vibrational response of cracked nanoplates and takes into account the flexoelectricity effect. Experiments conducted by Su *et al*. (2012) demonstrated conclusively that graphene oxide had viscoelastic characteristics. Srivastava *et al*. (2012) conducted research on the mechanical characteristics of graphene composites when they were subjected to dynamic loading. The researchers discovered that the graphene/epoxy and graphene/poly-dimethylsiloxane composites had viscoelastic features. Eichler *et al*. (2011) provided an illustration of the damping properties of mechanical resonators that were based on either a carbon nanotube or a graphene sheet. Consequently, taking into consideration the viscoelastic features of graphene is necessary in order to get conclusions that are more realistic about the behavior of graphene sheets. Pouresmaeeli *et al*. (2013) analyzed the free vibration of an orthotropic single-layered graphene sheet over a Kelvin–Voigt viscoelastic substrate using the classical plate theory. This was part of a larger theoretical research on viscoelastic nanostructures. Eringen's nonlocal theory is utilized to account for small-scale effects. Doan *et al*. (2022) analyze the vibration and static buckling of flexoelectric nano-plates. Karlicic *et al*. (2014) employed nonlocal continuum theory to study the natural transverse frequency of multi-layered viscoelastic nanoplates embedded in a viscoelastic foundation. Karlicic *et al*. (2015) used clampedclamped and clamped-free boundary conditions to illustrate longitudinal nanorod vibration. Hashemi *et al*. (2015) used the Kirchhoff plate theory to calculate an orthotropic bilayer graphene system's nonlocal natural frequency in a visco-Pasternak medium. Wang *et al*. (2015) studied bilayer graphene's nonlinear vibration using Galerkin's method. In the aforesaid study, nanostructure materials are represented

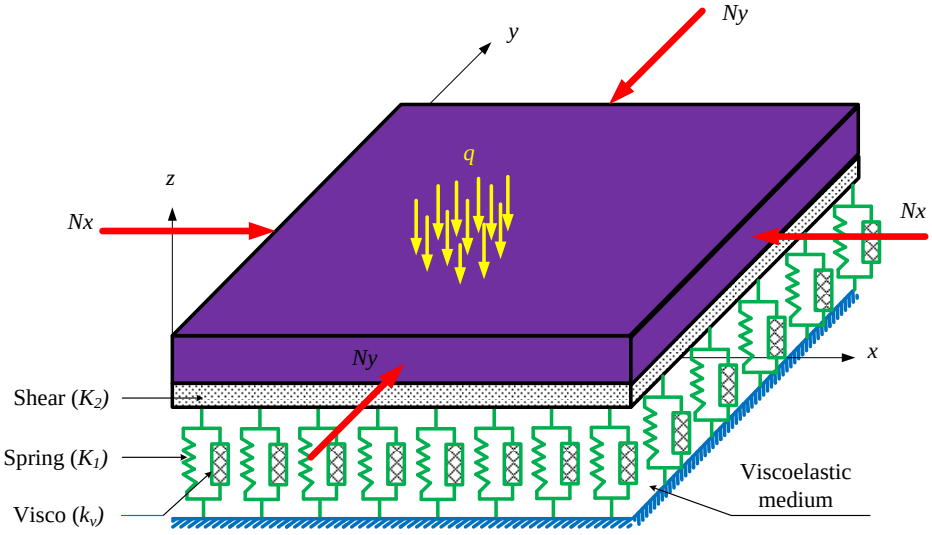

Fig. 1 The model of a nanoplate resting on a viscoelastic foundation subjected to multiple loads

using a modified Kelvin–Voigt relation for viscoelasticity. Akbas (2016-2019) combined a modified version of the couple stress theory with the Kelvin–Voigt viscoelastic model to examine the vibration response of a complete and fragmented viscoelastic nanobeam on a Winkler–Pasternak elastic foundation. Demir and Oz (2014) used finite elements to study a FG beam under viscoelastic conditions. Ebrahimi *et al*. 2019d used the Euler–Bernoulli beam model and Eringen's nonlocal theory to study curved magneto-electro-viscoelastic FG nanobeams on viscoelastic foundations. In addition, numerous studies on the mechanical performance of beams, plates, and shell structures have been carried out as of late, with some examples of typical applications including the following: (Pham *et al*. 2016, Tinh *et al*. 2016, Quang *et al*. 2022, Hoang-Nam *et al*. 2019a, b, Ebrahimi *et al*. 2019b, c, Nam *et al*. 2019, Thom *et al*. 2020, 2022, Singh *et al*. 2021, Abdelaziz 2021, Luat *et al*. 2021, Zhang *et al*. 2022, Foroutan and Dai 2022, Zhou 2022, Wenjuan 2022, Zhonghong and Gongxing 2022, Jinxuan *et al*. 2022, Xiao *et al*. 2022, Jing-Lei *et al*. 2022, Minh and Thanh 2022, Thanh *et al*. 2022, Cuong-Le *et al*. 2021, Tuan *et al*. 2021, Tho *et al*. 2023, Duc *et al*. 2018a, Tran *et al*. 2020, Tien *et al*. 2023, Pham *et al*. 2022, Nguyen *et al*. 2019, Thom *et al*. 2017, Duc *et al*. 2018b, Bui 2022, 2023, Tuyen 2023, Bui and Gia 2023, Lieu and Gia 2023, Ahmed-Amine *et al*. 2022, Mahmoud *et al*. 2022, Aissa *et al*. 2022, Wenjuan 2022, Zhe *et al*. 2022, Smain *et al*. 2022, Lingao 2022, Zhonghong and Gongxing 2022, Jinxuan *et al*. 2022, Xiao *et al*. 2022, Jing-Lei *et al*. 2022).

It is easy to see, through the works that have been published, that there has not been any research showing that the free vibration and static bending response of nano-structures resting on viscoelastic substrates have taken into account the flexoelectricity effect and the size effect. This demonstrates that the size effect cannot be ignored when calculating nanostructures with the flexoelectricity effect. In order to provide a solution to this issue, the authors of this work apply a mixture of Mindlin's theory and analytical approaches.

The remaining parts of this work are organized as described below. In the second section, which also takes into account the flexoelectricity effect and the axial compressive force, a comprehensive presentation of the equilibrium equation of the nanostructure is given. The third section gives an analytical solution for finding the natural and bending frequencies of nanostructure. In section 4, instances of verification are shown to the reader. Section 5 contains a substantial amount of commentary in addition to the numerical data. In conclusion, Section 6 summarizes the most significant findings from the preceding excursions of this study.

2. Equilibrium equations of nanoplates based on nonlocal theory

Computing the free vibration and the static bending behaviors of the modeled nanoplate illustrated in Fig. 1 is the primary emphasis of this body of work. Compressed in the *Oxy* plane by compressive loads N_x and N_y, the nanoplate also has the perpendicular coordinate systems of *Oxyz*, and the load *q* acts perpendicular to the plane of the plate. The geometric dimensions of the plate are *a* and *b*, while the plate thickness is *h*.

Assuming that the nanoplate satisfies Mindlin's first-order shear deformation theory, now, the three displacement components along the three coordinate axes respectively *Ox*, *Oy* and *Oz* at any point with coordinates (*x*, *y*, *z*) are represented as follows (Phung *et al*. 2022, Reissner (1985):

$$\begin{cases} u(x,y,z,t) = u_0(x,y,0,t) + z\varphi_x \\ v(x,y,z,t) = v_0(x,y,0,t) + z\varphi_y \\ w(x,y,z,t) = w(x,y,t) \end{cases} \quad (1)$$

where *u*, *v*, and *w* are the components of the vertical displacements in the three directions *Ox*, *Oy*, and *Oz* at the point with coordinates (*x*, *y*, *z*), and u_0 and v_0 are the two

displacements at the mean plane of the plate ($z = 0$).

Derivative of the variables x, y, and z, one gets the components of bending strain and shear strain in the following form:

$$\begin{cases} \varepsilon = \varepsilon_m + z\varepsilon_k \\ \gamma = \gamma_0 \end{cases} \tag{2}$$

where

$$\begin{aligned} \varepsilon_m &= \{\varepsilon_{mx}, \varepsilon_{my}, \gamma_{mxy}\}^T;\ \varepsilon_k = \{\varepsilon_{kx}, \varepsilon_{ky}, \varepsilon_{kxy}\}^T;\ \gamma_0 \\ &= \{\gamma_{xz}, \gamma_{yz}\}^T \\ \varepsilon_{mx} &= \frac{\partial u_0}{\partial x};\ \varepsilon_{my} = \frac{\partial v_0}{\partial y};\ \varepsilon_{kx} = \frac{\partial \varphi_x}{\partial x};\ \varepsilon_{ky} = \frac{\partial \varphi_y}{\partial y} \\ \gamma_{mxy} &= \frac{\partial u_0}{\partial y} + \frac{\partial v_0}{\partial x};\ \varepsilon_{kxy} = \left(\frac{\partial \varphi_x}{\partial y} + \frac{\partial \varphi_y}{\partial x}\right);\ \gamma_{xz} \\ &= \varphi_x + \frac{\partial w}{\partial x};\ \gamma_{yz} = \varphi_y + \frac{\partial w}{\partial y} \end{aligned} \tag{3}$$

Due to the influence of the flexoelectricity effect, it is necessary to take into account the strain gradient, which has the following expression:

$$\eta = \begin{Bmatrix} \eta_{xxz} = \dfrac{\partial \varepsilon_x}{\partial z} = \dfrac{\partial \varphi_x}{\partial x} \\ \eta_{yyz} = \dfrac{\partial \varepsilon_y}{\partial z} = \dfrac{\partial \varphi_y}{\partial y} \end{Bmatrix} \tag{4}$$

In this particular investigation, the strain gradient along the z-axis is not taken into consideration; rather, only those along the x- and y-axes are investigated. This suggests that the strain gradients along the x and y axes are much greater than those in the thickness direction (Tho *et al*. 2021, Thai *et al*. 2022).

When dealing with nanoscale structures, it is essential to take into account the size effect. There are many various theories that may be used to quantify this effect; however, the theory that is utilized in this work is the one that incorporates the nonlocal scale coefficient l. This coefficient is also the parameter that represents the small scale influence on nanoscale structures. When the flexoelectric effect is taken into account, the following formulation may be used to describe the stress components and electric displacement vector for a nanoscale dielectric material (Tho *et al*. 2021, Thai *et al*. 2022, Doan *et al*. 2022, Aghababaei and Reddy 2009):

$$\begin{aligned} &(1 - l^2\nabla^2)\sigma_{ij} = c_{ijkl}\varepsilon_{kl} - e_{kij}E_k; \\ &(1 - l^2\nabla^2)\tau_{mn} = c_{mn}\gamma_{mn} \\ &L_{ijm} = -f_{kijm}E_k \\ &Q_i = c_{ijk}\varepsilon_{jk} + \kappa_{ij}E_k + f_{ijkl}\eta_{jkl} \end{aligned} \tag{5}$$

where ∇^2 represents the Laplacian and σ_{ij} indicates the stress tensor, which has properties that are analogous to those of the conventional elastic substrate. $c_{ijkl}, e_{kij}, f_{kijm}$ and κ_{ij} are the parts of elastic, piezoelectric, flexoelectric, and permittivity constant tensors; they are also the material parameters. L_{ijm} is the moment stress tensor or the higher-order stress tensor, and Q_i is the electric displacement vector.

It is presumed that the only direction in which the electric field can act on the plate is in the direction that is perpendicular to the plane of the plate, which is the direction that points toward Oz (Tho *et al*. 2021, Thai *et al*. 2022, Doan *et al*. 2022). Therefore, in order to compute the electric field E_z, the derivative of the electrical potential H must first be used.

$$E_z = -\frac{\partial H}{\partial z} \tag{6}$$

One obtains, in accordance with the law of Gaussian:

$$\frac{\partial Q_z}{\partial z} = 0 \tag{7}$$

From Eqs. (5)-(7), the electric field expression E_z is found to have the following form:

$$E_z = z\frac{e_{31}}{k_{33}}\left(\frac{\partial^2 w}{\partial x^2} + \frac{\partial^2 w}{\partial y^2}\right) + E_0 \tag{8}$$

Since E_0 is a constant, the following boundary condition is required in order to find this constant as well as the precise expression of E_z:

$$Q_z\left(\pm\frac{h}{2}\right) = 0 \tag{9}$$

Eq. (9) gives the expression of E_z as follows:

$$\begin{aligned} E_z = &-\frac{e_{31}}{k_{33}}\left(\frac{\partial \varphi_x}{\partial x} + \frac{\partial \varphi_y}{\partial x}\right)z - \frac{e_{31}}{k_{33}}\left(\frac{\partial u_0}{\partial x} + \frac{\partial v_0}{\partial y}\right) \\ &- \frac{f_{14}}{k_{33}}\left(\frac{\partial \varphi_x}{\partial x} + \frac{\partial \varphi_y}{\partial y}\right) \end{aligned} \tag{10}$$

The components in expression (5) can be specifically expanded as follows:

$$\begin{aligned} (1 - l^2\nabla^2)\sigma &= (1 - l^2\nabla^2)\begin{Bmatrix} \sigma_x \\ \sigma_y \\ \tau_{xy} \end{Bmatrix} \\ &= \begin{bmatrix} c_{11} & c_{12} & 0 \\ c_{12} & c_{11} & 0 \\ 0 & 0 & c_{66} \end{bmatrix}\begin{Bmatrix} \varepsilon_x \\ \varepsilon_y \\ \gamma_{xy} \end{Bmatrix} - e_{31}\begin{Bmatrix} 1 \\ 1 \\ 0 \end{Bmatrix}E_z \end{aligned} \tag{11}$$

$$\begin{aligned} &(1 - l^2\nabla^2)\tau = (1 - l^2\nabla^2)\begin{Bmatrix} \tau_{xz} \\ \tau_{yz} \end{Bmatrix} = \begin{bmatrix} c_{66} & 0 \\ 0 & c_{66} \end{bmatrix}\begin{Bmatrix} \gamma_{xz} \\ \gamma_{yz} \end{Bmatrix}; \\ &L = \begin{Bmatrix} L_{xxz} \\ L_{yyz} \end{Bmatrix} = -f_{14}\begin{Bmatrix} 1 \\ 1 \end{Bmatrix}E_z \end{aligned} \tag{12}$$

$$Q_z = e_{31}(\varepsilon_{xx} + \varepsilon_{yy}) + \kappa_{33}E_z + f_{14}(\eta_{xxz} + \eta_{yyz}) \tag{13}$$

in which $f_{14} = f_{3113}$ and $f_{14} = f_{3223}$ (Shu *et al*. 2011, Thai *et al*. 2022, Doan *et al*. 2022) .

The internal force components including resultant forces (F_x, F_y, F_{xy}), resultant moments (M_x, M_y, M_{xy}) and shear force components (Q_{xz}, Q_{yz}) are calculated through the integration of the thickness variable as follows:

$$\begin{aligned} &\left\{\begin{Bmatrix} F_x \\ F_y \\ F_{xy} \end{Bmatrix}, \begin{Bmatrix} M_x \\ M_y \\ M_{xy} \end{Bmatrix}\right\} = \int_{-h/2}^{h/2} \sigma\{1, z\}dz = \\ &\int_{-h/2}^{h/2} \begin{Bmatrix} \sigma_x \\ \sigma_y \\ \tau_{xy} \end{Bmatrix}\{1, z\}dz; \end{aligned} \tag{14}$$

$$\begin{Bmatrix} Q_{xz} \\ Q_{yz} \end{Bmatrix} = \frac{5}{6}\int_{-h/2}^{h/2} \tau dz = \frac{5}{6}\int_{-h/2}^{h/2} \begin{Bmatrix} \tau_{xz} \\ \tau_{yz} \end{Bmatrix} dz$$

With stress components as illustrated in Eq. (11), the integrals in Eq. (14) take the following particular form:

$$\begin{aligned} &\begin{Bmatrix} F_x \\ F_y \\ F_{xy} \end{Bmatrix} - l^2\nabla^2 \begin{Bmatrix} F_x \\ F_y \\ F_{xy} \end{Bmatrix} = \int_{-\frac{h}{2}}^{\frac{h}{2}} \begin{Bmatrix} c_{11}\varepsilon_x + c_{12}\varepsilon_y \\ c_{11}\varepsilon_y + c_{12}\varepsilon_x \\ c_{66}\gamma_{xy} \end{Bmatrix} dz \\ &+e_{31}\int_{-h/2}^{h/2} \begin{Bmatrix} \frac{e_{31}}{k_{33}}\left(\frac{\partial u_0}{\partial x} + \frac{\partial v_0}{\partial y}\right) - \frac{f_{14}}{k_{33}}\left(\frac{\partial \varphi_x}{\partial x} + \frac{\partial \varphi_y}{\partial y}\right) \\ \frac{e_{31}}{k_{33}}\left(\frac{\partial u_0}{\partial x} + \frac{\partial v_0}{\partial y}\right) - \frac{f_{14}}{k_{33}}\left(\frac{\partial \varphi_x}{\partial x} + \frac{\partial \varphi_y}{\partial y}\right) \\ 0 \end{Bmatrix} dz \end{aligned} \tag{15a}$$

$$\begin{aligned} &\begin{Bmatrix} M_x \\ M_y \\ M_{xy} \end{Bmatrix} - l^2\nabla^2 \begin{Bmatrix} M_x \\ M_y \\ M_{xy} \end{Bmatrix} \\ &= \int_{-\frac{h}{2}}^{\frac{h}{2}} \begin{Bmatrix} c_{11}\varepsilon_x + c_{12}\varepsilon_y \\ c_{11}\varepsilon_y + c_{12}\varepsilon_x \\ c_{66}\gamma_{xy} \end{Bmatrix} z dz \\ &+e_{31}\int_{-h/2}^{h/2} \begin{Bmatrix} \frac{e_{31}}{k_{33}}\left(\frac{\partial \varphi_x}{\partial x} + \frac{\partial \varphi_y}{\partial x}\right) \\ \frac{e_{31}}{k_{33}}\left(\frac{\partial \varphi_x}{\partial x} + \frac{\partial \varphi_y}{\partial x}\right) \\ 0 \end{Bmatrix} z^2 dz \end{aligned} \tag{15b}$$

$$\begin{aligned} &\begin{Bmatrix} Q_{xz} \\ Q_{yz} \end{Bmatrix} - l^2\nabla^2 \begin{Bmatrix} Q_{xz} \\ Q_{yz} \end{Bmatrix} = \frac{5}{6}\int_{-\frac{h}{2}}^{\frac{h}{2}} \begin{Bmatrix} \tau_{xz} \\ \tau_{yz} \end{Bmatrix} dz \\ &= \frac{5}{6}\int_{-h/2}^{h/2} c_{66} \begin{Bmatrix} \gamma_{xz} \\ \gamma_{yz} \end{Bmatrix} dz \end{aligned} \tag{15c}$$

Therefore, the expressions in Equation (15) show that the internal force components of the nanoplate, in the case of taking into account the flexoelectricity effect, will appear to have some other components than those of the ordinary nanostructure. This is because the flexoelectricity effect causes the nanoplate to deform in a way that makes it more flexible. This also results in the plate's equilibrium equation becoming more difficult, and the plate's mechanical reaction becoming distinct from the response of a conventional nanostructure.

In addition to the numerous research that have been conducted on structures that are based on elastic foundations, there are also various computational models for elastic foundations. Nevertheless, there are circumstances in which it can be regarded as a viscoelastic foundation model. During these instances, there is an additional coefficient of viscous resistance of the foundation; consequently, the force that is exerted by the viscous foundation on the plate is determined by the formula Zenkour (2016), which is as follows:

$$P_V = \left(k_1 - k_2\nabla^2 + k_v\frac{\partial}{\partial t}\right)w \tag{16}$$

where the damping drag coefficient of the viscoelastic medium is denoted by k_v and the time variable is denoted by t, $\nabla^2 = \frac{\partial^2}{x^2} + \frac{\partial^2}{y^2}$. Because of this, drawing the conclusion that the normal elastic foundation is just a specific case when the viscous drag coefficient is omitted is a simple and straightforward process.

The following are the various forms that the work that can be done by the inertial force can take:

$$\begin{aligned} \delta K &= \int_A \int_{-h/2}^{h/2} \rho \left\{ \left(\frac{\partial^2 u}{\partial t^2}\right)\delta u + \left(\frac{\partial^2 v}{\partial t^2}\right)\delta v + \left(\frac{\partial^2 w}{\partial t^2}\right)\delta w \right\} dz dA \\ &= \int_A \int_{-h/2}^{h/2} \rho \begin{Bmatrix} \left(\frac{\partial^2 u_0}{\partial t^2}\right)\delta u_0 + \left(\frac{\partial^2 v_0}{\partial t^2}\right)\delta v_0 \\ +\left(\frac{\partial^2 \varphi_x}{\partial t^2}\right) z^2 \delta\varphi_x \\ +\left(\frac{\partial^2 \varphi_y}{\partial t^2}\right) z^2 \delta\varphi_y + \left(\frac{\partial^2 w}{\partial t^2}\right)\delta w \end{Bmatrix} \delta w dz dA \end{aligned} \tag{17}$$

The possible work of P_V force due to the action of viscoelastic foundation has the following expression:

$$\begin{aligned} \delta\Pi_v &= \int_A P_v \delta w dS \\ &= \int_A \left(k_1 w - k_2\nabla^2 w + k_v\frac{\partial w}{\partial t}\right)\delta w dA \end{aligned} \tag{18}$$

The expression for the possible work of the external force acting on the plate has the following expression:

$$\delta\Pi_{force} = \int_A \left\{ q + N_x\frac{\partial w}{\partial x}\frac{\partial \delta w}{\partial x} + N_y\frac{\partial w}{\partial y}\frac{\partial \delta w}{\partial y} \right\}\delta w dA \tag{19}$$

where q is the force acting perpendicular to the plane of the plate, and N_x and N_y are the compressive forces acting in the plane of the plate.

The possible work of the internal force of the plate has the form:

$$\begin{aligned} &\delta\Pi_e \\ &= \int_A \int_{-h/2}^{h/2} \begin{pmatrix} \sigma_x\delta\varepsilon_x + \sigma_y\delta\varepsilon_y + \tau_{xy}\delta\gamma_{xy} \\ +\tau_{xz}\delta\gamma_{xz} + \tau_{yz}\delta\gamma_{yz} + L_{xxz}\delta\eta_{xxz} \\ +L_{yyz}\delta\eta_{yyz} \end{pmatrix} dz dA \end{aligned} \tag{20}$$

The following is the particular form that the equilibrium equation of the nanoplate takes after being established on the basis of Hamilton's principle:

$$\int_{t_0}^{t_1} (\delta K - \delta\Pi_e - \delta\Pi_v - \delta\Pi_{force}) dt = 0 \tag{21}$$

Following is a list of the five balanced equations that may be derived from Equation (20):

$$\delta u_0\colon \frac{\partial F_x}{\partial x} + \frac{\partial F_{xy}}{\partial y} = (1 - l^2\nabla^2)\rho h\frac{\partial^2 u_0}{\partial t^2} \tag{22}$$

$$\delta v_0\colon \frac{\partial F_y}{\partial y} + \frac{\partial F_{xy}}{\partial x} = (1 - l^2\nabla^2)\rho h\frac{\partial^2 v_0}{\partial t^2} \tag{23}$$

$$\delta\varphi_x\colon \frac{\partial M_x}{\partial x} + \frac{\partial M_{xy}}{\partial x} + Q_{xz} + B_{fx} + (1 - l^2\nabla^2)\rho\frac{h^3}{12}\frac{\partial^2\varphi_x}{\partial t^2} = 0 \tag{24}$$

$$\delta\varphi_y\colon \frac{\partial M_{xy}}{\partial y} + \frac{\partial M_y}{\partial y} + Q_{yz} + B_{fy} + (1 - l^2\nabla^2)\rho\frac{h^3}{12}\frac{\partial^2\varphi_x}{\partial t^2} = 0 \tag{25}$$

$$\delta w:\ \frac{\partial Q_{xz}}{\partial x}+\frac{\partial Q_{yz}}{\partial y}-(1-l^2\nabla^2)\begin{Bmatrix} q-k_1 w+k_2\nabla^2 w-k_v\frac{\partial w}{\partial t} \\ -\left\{N_x\frac{\partial^2 w}{\partial x^2}+N_y\frac{\partial^2 w}{\partial y^2}\right\}\end{Bmatrix} = (1-l^2\nabla^2)\rho h\frac{\partial^2 w}{\partial t^2} \tag{26}$$

where

$$B_{fx}=\int_{-h/2}^{h/2} L_{xxz}dz;\ B_{fy}=\int_{-h/2}^{h/2} L_{yyz}dz \tag{27}$$

For the SSSS nanoplate, boundary conditions for the plate include:

$$\begin{aligned} &w(x,0,t)=w(x,b,t)\\ &=w(0,y,t)=w(a,y,t)=0\\ &\varphi_x(x,0,t)=\varphi_x(x,b,t)\\ &=\varphi_y(0,y,t)=\varphi_y(a,y,t)=0\\ &M_x(0,y,t)=M_x(a,y,t)\\ &=M_y(x,0,t)=M_y(x,b,t)=0 \end{aligned} \tag{28}$$

3. Analytical solutions to the problem of free vibrations and static bending of nanoplates

The objective is to identify the unknown values for each of the five problems by applying the exact solution to each of the associated Eqs. (22)-(26). In order to tackle the problem, this work applies analytical approaches, which involve combining the Fourier transform in the *x* and *y* directions with the Fourier transform in time *t*. For the free vibration problem, if one disregards the applied force *q*, the following are the solutions that may be discovered for the five different displacement components:

$$\begin{aligned} u_0(x,y,t)&=U_{0x}\sin\left(\frac{\pi x}{a}\right)\cos\left(\frac{\pi y}{b}\right)e^{-i\omega t}\\ v_0(x,y,t)&=V_{0y}\cos\left(\frac{\pi x}{a}\right)\sin\left(\frac{\pi y}{b}\right)e^{-i\omega t}\\ w(x,y,t)&=W_0\sin\left(\frac{\pi x}{a}\right)\sin\left(\frac{\pi y}{b}\right)e^{-i\omega t}\\ \varphi_x(x,y,t)&=\Phi_{0x}\cos\left(\frac{\pi x}{a}\right)\sin\left(\frac{\pi y}{b}\right)e^{-i\omega t}\\ \varphi_y(x,y,t)&=\Phi_{0y}\sin\left(\frac{\pi x}{a}\right)\cos\left(\frac{\pi y}{b}\right)e^{-i\omega t} \end{aligned} \tag{29}$$

in which i^2 = -1 and ω is the fundamental circular frequency.

When Eqs. (22) through (26) are solved using the solution form (29), one obtains the equation for finding the natural frequency of oscillation of the plate, which has the following general form:

$$\omega=\omega_{re}+i\omega_{im} \tag{30}$$

where ω_{re} and ω_{im} are the real and imaginary parts of the natural frequency of the nanoplate.

For the bending issue involving nanostructures, the solution form of the displacement components of the plate has the following specifications when the density component is disregarded in the equilibrium Eqs. (22)-(26):

$$\begin{aligned} w(x,y,t)&=W\sin\left(\frac{\pi x}{a}\right)\sin\left(\frac{\pi y}{b}\right)^{\Omega t}_{\ max}\\ \varphi_x(x,y,t)&=\Phi\cos\left(\frac{\pi x}{a}\right)\sin\left(\frac{\pi y}{b}\right)^{\Omega t}_{\ xmax}\\ \varphi_y(x,y,t)&=\Phi\sin\left(\frac{\pi x}{a}\right)\cos\left(\frac{\pi y}{b}\right)^{\Omega t}_{\ ymax}\\ u_0(x,y,t)&=U\sin\left(\frac{\pi x}{a}\right)\cos\left(\frac{\pi y}{b}\right)^{\Omega t}_{\ xmax}\\ v_0(x,y,t)&=V\cos\left(\frac{\pi x}{a}\right)\sin\left(\frac{\pi y}{b}\right)^{\Omega t}_{\ ymax}\\ q(x,y,t)&=\frac{16Q_{max}}{\pi^2\sin\left(\frac{\pi x}{a}\right)\sin\left(\frac{\pi y}{b}\right)^{\Omega t}} \end{aligned} \tag{31}$$

in which Ω is the angular frequency.

Substituting the solution expression (31) into the balanced Eqs. (22)-(26), it is easy to derive the solution expression $W_{\max}$, Φ_{xmax}, Φ_{ymax}, U_{xmax} and V_{ymax}, which are functions of the angular frequency Ω.

The expression of the natural vibrational frequency and displacement of the nanoplate has sufficient components related to the nonlocal parameter *l*, the coefficient of the viscoelastic foundation, the coefficients showing the effect of the flexoelectricity effect, and the two compressive force components acting on the nanoplate, as shown by the above calculation expressions. If the flexoelectricity effect is disregarded, the natural frequency of the plate will return to the normal nanosheet, and due to the appearance of the viscous drag coefficient of the elastic matrix, there will be a coefficient associated with the imaginary component, which in general will have both real and imaginary components.

4. Verification examples

This part performs four instances to evaluate the accuracy of the proposed theory and mathematical models. The numerical data of these examples are compared with those of other reliable publications.

Verification problem 1: This is a plate with dimensions *a*/*b*=1 and the thickness *h*=*a*/20, which is fully supported (SSSS). *E*=380 Gpa, ρ = 3800 kg/m^3, and ν = 0.3 are the plate's material characteristics. The plate is supported by an elastic base, which has two parameters:

$$K_w^*=\frac{k_1 a^4}{D_0};\ K_s^*=\frac{k_2 a^2}{D_0} \tag{32}$$

in which $D_0=\frac{E_0 h^3}{12(1-\nu^2)}$; E_0=70 GPa.

The following formula normalizes the plate's first non-dimensional fundamental frequency:

$$\varpi=\omega h\sqrt{\rho_0/E_0};\ \rho_0=2707\ (\text{kg/m}^3) \tag{33}$$

The comparative non-dimensional fundamental frequencies of the plate determined by this work and the analytical solution (Baferani *et al*. 2011) are provided in Table 1. It can be concluded that the comparative results illustrate the reliability of this study.

Table 1 The non-dimensional natural frequency ϖ of the plate resting on an elastic foundation

K_w^*	K_s^*	Baferani *et al*. 2011	This work
0	0	0.0292	0.0294
0	100	0.0407	0.0408
100	0	0.0299	0.0301
100	100	0.0412	0.0413

Table 2 The comparative natural frequency $\breve{\omega}$ of the nanoplate taking into account the nonlocal parameter *l*

a/*b*	*a*/*h*	*l* (nm)	This work	Aghababaei and Reddy (2009)
1	10	0	0.0937	0.0935
		1	0.0856	0.0854
	20	0	0.0239	0.0239
		1	0.0218	0.0218
2	10	0	0.0579	0.0591
		1	0.0546	0.0557
	20	0	0.0146	0.0150
		1	0.0138	0.0141

Table 3 The comparative deflection $\breve{w}$ of the nanoplate taking into account the nonlocal parameter *l*

a/*h*	*l* (nm)	This work	Aghababaei and Reddy (2009)
50	0	4.1700	4.0154
	0.5	4.3758	4.3779
	1	4.9931	4.7404
100	0	4.1629	4.0100
	0.5	4.3684	4.3721
	1	4.9847	4.7342

Verification problem 2: In this problem, a fully simply supported nanoplate with geometrical and material characteristics: h=20 nm, a=b=50h, c_{11}=102 GPa; c_{12}=31 GPa; c_{33}=35.50 GPa; e_{31}=-17.05 C/m^2; k_{33}=1.76.10^{-8} C/(Vm); f_{14}=10^{-7} C/m, and mass density 7600 kg/m^3 is taken into calculation. When using Yang *et al*. 2015's analytical formulation, the first fundamental frequency is calculated to be 4.7638.10^8 rad/s. The proposed theory and mathematical model have been proven to be correct by the comparison of their results.

Verification problem 3: This example illustrates the natural frequency of nanostructure under the effect of the nonlocal parameter *l*. Let us consider an SSSS square nanoplate with dimensions of a = b = 10 nm, thicknesses of h = a/10 and a/20, Young's modulus E = 30 MPa, Poisson's ratio ν = 0.3, and mass density ρ = 1. The first natural frequency of the plate is calculated by the formula $\breve{\omega} = \omega h\sqrt{\rho/G}$, where $G = E/\big(2(1+\nu)\big)$. The results of calculating the natural frequency of the nanosheets are compared as shown in Table 2. Since then, one can see the reliability of this work has been verified.

Verification problem 4: This instance examines the nanoplate's deflection while accounting for the effect of the nonlocal parameter l. Consider an SSSS nanoplate with the following geometric and material parameters: a = b = 10 nm, h = a/50 and a/100, E = 30 MPa, Poisson's ratio ν = 0.3, and Q_0 = 1. Using the formula $\breve{w} = 10^3 h^3 w(12(1-\nu^2)Q_0 a^4)_{max}$, the static deflection of the plate is determined. The Table 3 comparison results indicate the necessary dependability of the theory of computing in this work.

5. Numerical results

On the basis of the theoretical calculation presented previously, this section will present the results of numerical calculations to show the influence of foundation parameters, materials, and the geometrical characteristics of the nano-plate on the free vibration and static bending responses of the nanostructure. The nano-plate has one side length a = 10 nm, and the other side b, the thickness h = a/20, and material properties are c_{11} = 102 GPa, e_{31}=-17.05 C/m^2; k_{33}=1.76.10^{-8} C/(Vm), mass densityρ = 7600 kg/m^3, f_{14}=10^{-7} C/m is valid in each specific calculation. The following formulas are used to normalize the non-dimensional frequency as well as the other parameters:

$\omega^* = 10\omega h_0\sqrt{\frac{\rho}{c_{11}}}$; $w* = \frac{100c_{11}h_0}{Q2_{max}\left(x=\frac{a}{2},y=\frac{b}{2}\right)}$; $k_1^* = \frac{12k_1a^4}{c_{11}h_0^3}$; $k_2^* = \frac{12k_2a^2}{\pi^2c_{11}h_0^3}$; $N_x^* = \frac{12N_{0x}a^2}{\pi^2c_{11}h_0^3}$; $N_y^* = \frac{12N_{0y}a^2}{\pi^2c_{11}h_0^3}$; $c_v^* = \frac{10^3k_v}{\sqrt{c_{11}\rho}}$; h_0 = 1 nm, $Q_{\max}$ = 0.05 MPa

5.1 Free vibration problem

Due to the viscoelastic medium, its inherent frequency is composed of both real and imaginary components. This section presents the findings of computing the real and imaginary components of the nanoplates's natural frequency for various material and load parameters. The results of computing the natural frequency response of the plate based on the parameter f_{14} and the nonlocal parameter *l* are shown in Table 4 (with and without the flexoelectricity effect). It was discovered that the flexoelectricity effect increased both the real and imaginary frequency components. The results indicate that the natural frequency of the plate increases as the value of f_{14} rises. This indicates that the flexoelectricity effect enhances the nanoplate's rigidity. In addition, as the value of f_{14} is increased, the imaginary part of the plate's natural frequency decreases. At the same time, when increasing the value of nonlocal parameter *l*, the real part of the natural frequency of the plate decreases. These computation findings also reveal that when the plate is evaluated using the nonlocal theory and the flexoelectricity effect is considered, the natural frequency of the nanosheets differs from the case computed using the classical theory (i.e., the parameter *l* is ignored). In other words, when computing nanosheets that include the flexoelecity effect, it is required to use the nonlocal theory, which yields more realistic results than neglecting the nonlocal parameter *l*.

Table 5 presents the findings of the calculation when both parameters f_{14} and k_v^* change. As the value of the

Table 4 The real part Real(ω) and the imaginary part Imag(ω) of the natural frequency of the nanoplate with the flexoelectricity effect ($f_{14} \neq 0$) and without the flexoelectricity effect (f_{14}=0), a/h =20, N_x^*=N_y^*=0.5, c_v^*= 10, k_1^* = 10, k_2^* = 4

	l (nm)	Without the flexoelectricity effect	With the flexoelectricity effect f_{14} (10^{-7} C/m)					
			0.4	1.0	1.4	2.0	3.0	4.0
Real(ω)	0	1.11170	1.78091	2.35833	2.47340	2.54444	2.58575	2.60082
	0.4	1.11043	1.76345	2.32951	2.44244	2.51217	2.55273	2.56753
	0.8	1.10701	1.71609	2.25093	2.35799	2.42413	2.46261	2.47666
	1	1.10480	1.68478	2.19867	2.30177	2.36550	2.40259	2.41613
Imag(ω)	0	0.10000	0.100683	0.100447	0.100277	0.100152	0.100071	0.100041
	0.4	0.10000	0.100681	0.100445	0.100276	0.100151	0.100071	0.100041
	0.8	0.10000	0.100676	0.100442	0.100274	0.100150	0.100071	0.100040
	1	0.10000	0.100671	0.100439	0.100272	0.100149	0.100070	0.100040

Table 5 The real part Real(ω) and the imaginary part Imag(ω) of the natural frequency of the nanoplate depending on f_{14} and the viscoelastic drag coefficient c_v^*, a/h =20, N_x^*=N_y^*= 0.5, k_1^* = 10, k_2^* = 4, l = 0.4 nm

	c_v^*	f_{14} (10^{-7} C/m)					
		0.4	1.0	1.4	2.0	3.0	4.0
Real(ω)	0	1.76631	2.33166	2.44449	2.51416	2.55469	2.56948
	10	1.76345	2.32951	2.44244	2.51217	2.55273	2.56753
	20	1.75484	2.32302	2.43627	2.50618	2.54684	2.56168
	40	1.71994	2.29692	2.41145	2.48209	2.52315	2.53814
Imag(ω)	0	0	0	0	0	0	0
	10	0.100681	0.100445	0.100276	0.100151	0.100071	0.100041
	20	0.201370	0.200894	0.200555	0.200304	0.200144	0.200082
	40	0.402789	0.401817	0.401127	0.400618	0.400292	0.400168

viscous drag coefficient k_v^* of the foundation steadily increases, the real portion of the plate's oscillation frequency lowers while the imaginary portion grows.

Table 6 presents the data of computing the natural frequency of the plate based on the ratio N_y^*/N_x^* and the viscoelastic parameter c_v^*. Table 6 demonstrates that as the ratio N_y^*/N_x^* increases, the real component of the nanoplate's natural frequency falls, whereas the imaginary component of the plate's natural frequency increases.

5.2 Static bending problem

In this part of the study, numerical findings for the deflection of the nanoplate while it is resting on the viscoelastic foundation are presented. This work provides two dimensionless parameters for the purposes of computation and study, as follows:

$$Re(w_{\mathrm{NL/L}}^*) = \frac{\mathrm{Real}\big(w_{\mathrm{NL}}(l \neq 0)\big)}{\mathrm{Real}\big(w_L(l = 0)\big)};$$

$$Im(w_{\mathrm{NL/L}}^*) = \frac{\mathrm{Im}\big(w_{\mathrm{NL}}(l \neq 0)\big)}{\mathrm{Im}\big(w_L(l = 0)\big)}$$

where w_{NL} represents the deflection$w\left(x = \frac{a}{2}, y = \frac{b}{2}\right)$ for the situation in which the non-zero parameter l is taken into account, and w_{L} denotes the deflection for the case in which the parameter l is ignored (l = 0). In this part of the calculation, the results will be adjusted so that the angular frequency Ω =0.5-0.1i.

Fig. 2 presents the data of computing the real and imaginary components of the nanoplate's defletion. This conclusion illustrates that the nonlocal parameter l is less the smaller the value of the coefficient f_{14}, the difference between the real and imaginary components of the defletion of the plate when the nonlocal parameter l is considered vs when it is ignored. The disparity increases as the value of the coefficient f_{14} increases. This demonstrates that when the coefficient f_{14} is greater, the flexoelectricity effect has a considerable impact on the displacement response of the plate. In addition, for each parameter l value, $Re(w_{\mathrm{NL/L}}^*)$ and $Im(w_{\mathrm{NL/L}}^*)$ vary nonlinearly and extensively as f_{14} takes on values between 0 and 10^{-7} C/m, but do not change much when f_{14} is more than 10^{-7} C/m. Furthermore, the calculation results demonstrate that as the nonlocal parameter l is larger, the difference between the theory of nonlocal computing and the conventional theory (ignoring parameter l) becomes more apparent. This implies that it is crucial to account for the effects of the nonlocal parameter on the nanoscale, particularly when considering the flexo-electrification effect.

Table 6 The real part Real(ω) and the imaginary part Imag(ω) of the natural frequency of the nanoplate depending on N_y^*/N_x^* and the viscoelastic drag coefficient c_v^*, f_{14} = 0.1x10^{-7} C/m, a/h =20, N_x^*= 0.5, k_1^* = 10, k_2^* = 4, l = 0.4 nm

	c_v^*	N_y^*/N_x^*					
		0	0.5	1.0	2.0	5.0	10
Real(ω)	0	1.22291	1.20626	1.18930	1.15463	1.04374	0.82648
	10	1.21889	1.20210	1.18508	1.15029	1.03893	0.82040
	20	1.20649	1.18954	1.17233	1.13715	1.02436	0.80187
	40	1.15559	1.13788	1.11988	1.08299	0.96388	0.72300
Imag(ω)	0	0	0	0	0	0	0
	10	0.100105	0.100105	0.100106	0.100106	0.100109	0.100113
	20	0.200211	0.200212	0.200213	0.200214	0.200219	0.200227
	40	0.400431	0.400433	0.400435	0.400438	0.400447	0.400464

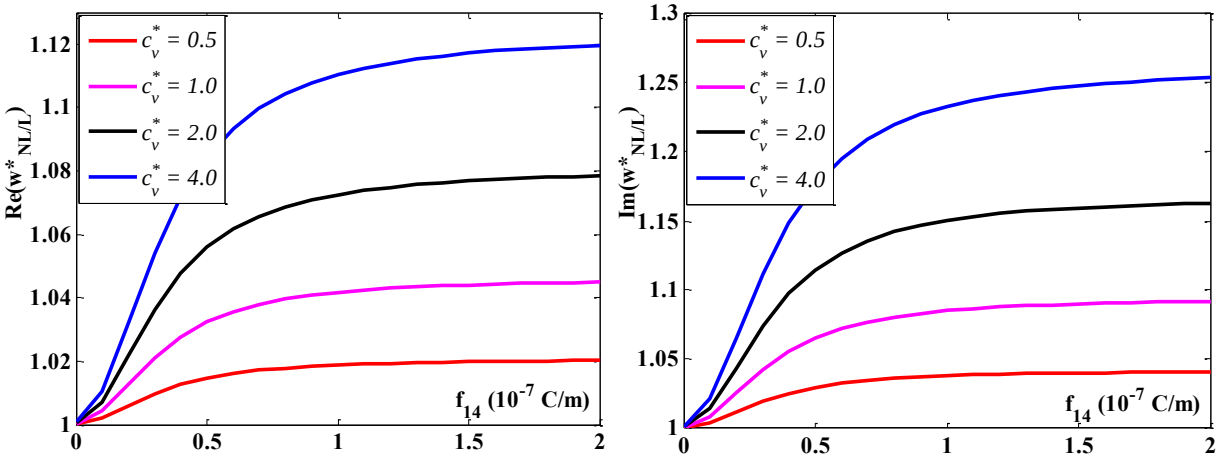

(a) $Re(w_{NL/L}^*)$ (b) $Im(w_{NL/L}^*)$

Fig. 2 The variation of the real and imaginary components of the deflection depending on f_{14} and the nonlocal parameter l, a/h =50, N_x^*=N_y^*= 0.5, k_1^* = 10, k_2^* = 4, c_v^* = 1, Ω =0.5 -0.1i

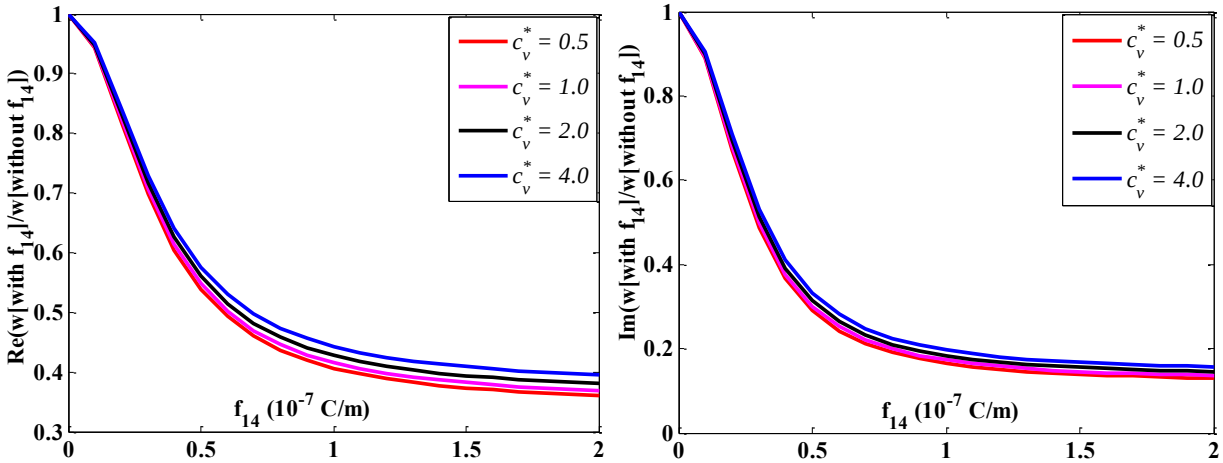

(a) $Re(w_{NL/L}^*)$ (b) $Im(w_{NL/L}^*)$

Fig. 3 The variation of the real and imaginary components of the deflection with the flexoelectricity effect (f_{14} ≠0) and without the flexoelectricity effect (f_{14}=0), a/h =50, N_x^*=N_y^*= 0.5, k_1^* = 10, k_2^* = 4, c_v^* = 1, Ω =0.5 -0.1i

Fig. 3 depicts the ratio of the real and imaginary components of displacement in the presence and absence of the flexoelectricity effect. The results of the calculations indicate that the flexoelectricity effect has made the plate

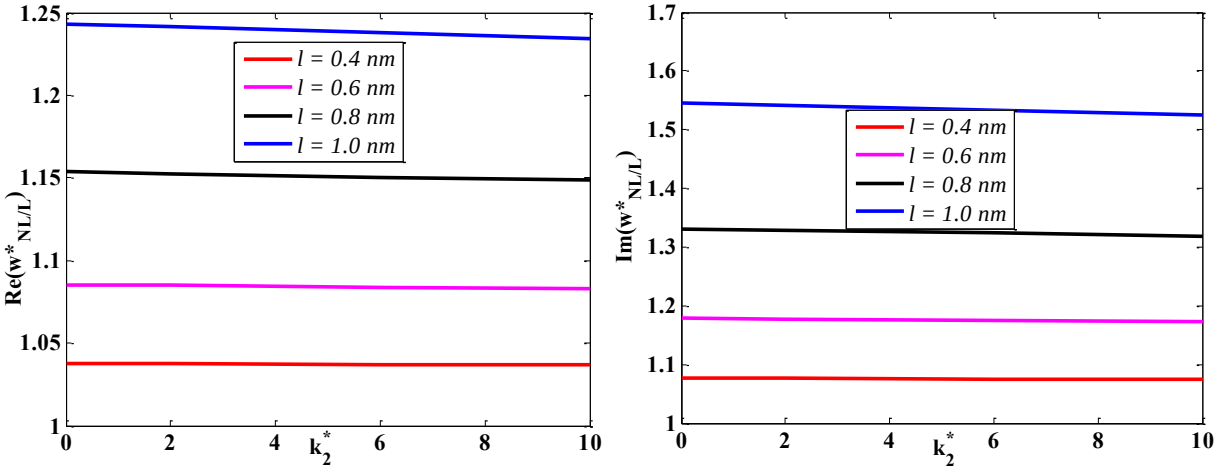

(a) $Re(w^*_{\mathrm{NL/L}})$ (b) $Im(w^*_{\mathrm{NL/L}})$

Fig. 4 The variation of the real and imaginary components of the deflection depending on f_{14} and the nonlocal parameter l, a/h =50, c_v^*= 1, k_1^*= 20,N_x^*=N_y^*= 0.5, f_{14} =0.5x10^{-7} C/m,Ω =0.5-0.1i

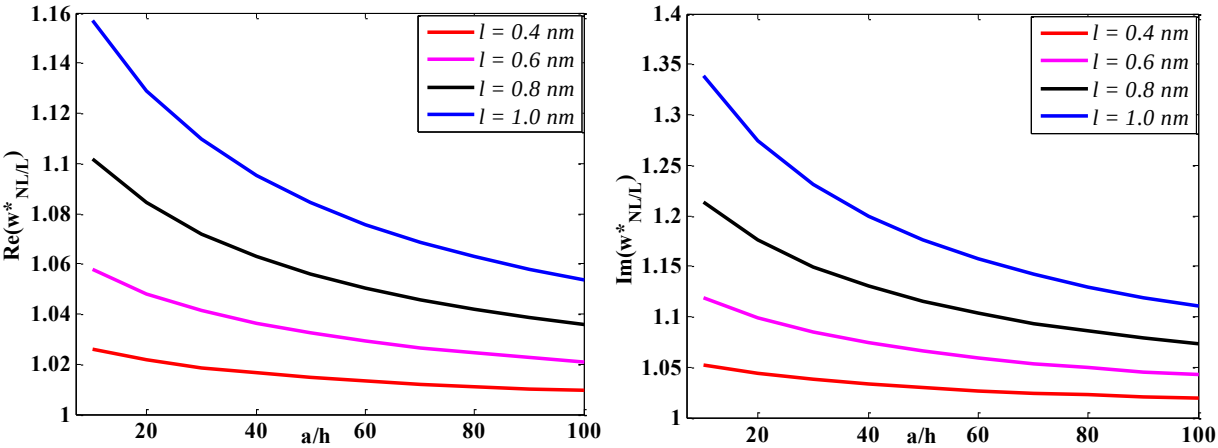

(a) $Re(w^*_{\mathrm{NL/L}})$ (b) $Im(w^*_{\mathrm{NL/L}})$

Fig. 5 The variation of the real and imaginary components of the deflection depending on a/h and the nonlocal parameter l, k_1^* = 10, k_2^* = 4, c_v^*= 1, N_x^*=N_y^*= 0.5, f_{14} =0.5x10^{-7} C/m, Ω =0.5-0.1i

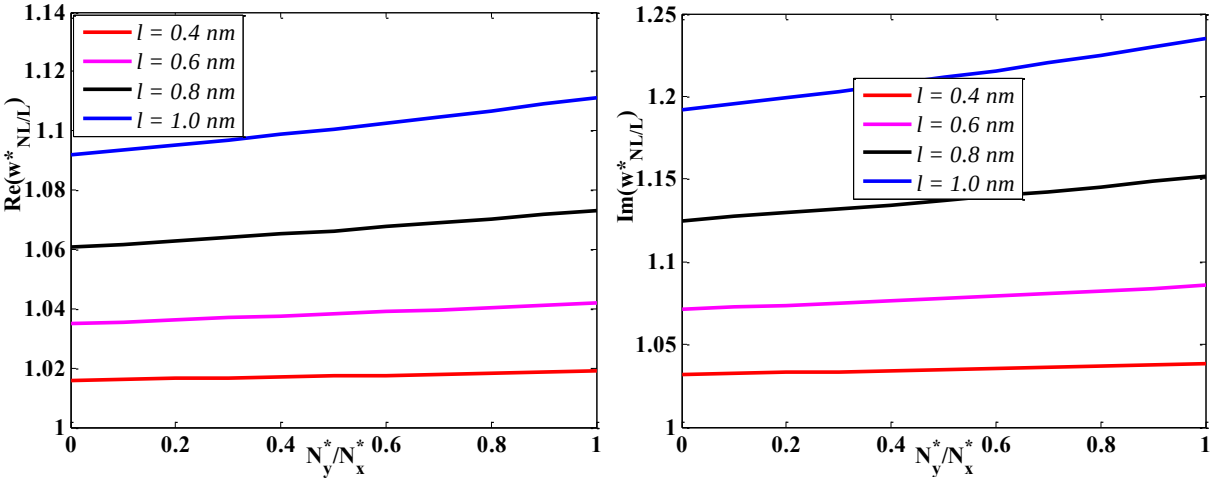

(a) $Re(w^*_{\mathrm{NL/L}})$ (b) $Im(w^*_{\mathrm{NL/L}})$

Fig. 6 The variation of the real and imaginary components of the deflection depending on N_y^*/N_x^* and the nonlocal parameter l, k_1 = 10, k_2 = 4, c_v^*= 1, k_1^*= 10, k_2^*= 4,N_x^*=2, f_{14} =0.5x10^{-7} C/m, Ω =0.5-0.1i

firmer, thereby increasing its load capacity.

Next, this work explores the effect of the substrate's elastic properties on the nanosheet's displacement response. The first foundation parameter k_1^* is fixed at 20 whereas the second parameter k_2^* changes between 0 and 10. Fig. 4 depicts the outcomes of calculations for $Re(w^*_{\mathrm{NL/L}})$ and $Im(w^*_{\mathrm{NL/L}})$. According to these results, the proportions of both the real and imaginary sections drop as the k_2^* value of the foundation increases for each value of the parameter *l*.

Fig. 5 shows the results of the estimates for $Re(w^*_{\mathrm{NL/L}})$ and $Im(w^*_{\mathrm{NL/L}})$ as the thickness *h* of the nanoplate varies. These are nonlinear curves; as the thickness of the plate decreases, $Re(w^*_{\mathrm{NL/L}})$ and $Im(w^*_{\mathrm{NL/L}})$ values decrease. This demonstrates that for each value of the nonlocal parameter *l*, the ratio of the real and imaginary components of the deflection is less when parameter *l* is considered compared to when parameter *l* is neglected.

The dependence of $Re(w^*_{\mathrm{NL/L}})$ and $Im(w^*_{\mathrm{NL/L}})$ on the ratio of compressive forces C/D acting on the plate is shown in Fig. 6. By seeing this figure, it is easy to see that, as the ratio of the compressive forces N_y^* / N_x^* increases, both$Re(w^*_{\mathrm{NL/L}})$and $Im(w^*_{\mathrm{NL/L}})$increase. This shows that for each value of the nonlocal parameter *l*, as the compression ratio increases, both the real and imaginary parts of the defelction when calculated in nonlocal theory are larger than the real and imaginary parts of the plate when the nonlocal parameter *l* is omitted.

6. Conclusions

This work presents for the first time the study of the free vibration and the static bending of the nanoplate resting on a viscoelastic foundation and taking into account the effect of the flexoelectricity effect. The plate is subjected to a simultaneous compressive load in the plate plane and a uniformly distributed load perpendicular to the surface of the plate. The work was accomplished by utilizing Mindlin's first-order shear deformation theory and analytical method. Both the natural frequency of the nanoplate and the bending deflection of this plate seem to have both real and imaginary components due to the viscoelastic features of the nanoplate. The computed findings also reveal that the flexoelecity effect raises the stiffness of the plate (through the coefficient f_{14}), which in turn raises the natural frequency of the plate. Concerning the bending issue of nanoplates, the flexoelectricity effect causes an increase in the difference between the real and imaginary portions in the scenario where nonlocal theory is used (with parameter *l*), in comparison to the scenario where nonlocal theory is not applied (ignore parameter *l*). When the nonlocal parameter *l* is given a large value, this disparity becomes more pronounced. One thing that this demonstrates is that when dealing with nanosheets that have the flexoelectricity effect, it is essential to take into account the effects of nonlocal parameters. The study presents intriguing findings, making it a useful scientific work for reference in the calculation, design, and application of nanoplates based on viscoelastic foundations and impacted by of the flexoelectricity effect. When it comes to this issue, the component that causes energy loss of the plate is the selection of the resistance parameter of the foundation. It is hoped that this work will serve as a foundation for future research into more intricate issues, such as the behavior of plates with fractures on viscous substrates and plates exposed to random loads in viscoelastic environments.

References

Abdelaziz, T. (2021), "A cylindrical shell model for nonlocal buckling behavior of CNTs embedded in an elastic foundation under the simultaneous effects of magnetic field, temperature change, and number of walls", *Adv. Nano. Res.*, **11**(6), 581-593. https://doi.org/10.12989/anr.2021.11.6.581

Aissa, K., Rabbab, B.B., Attia, B., Mohamed, S., Samir, B., Mahmoud, M.S.S., Tounsi, A. and Muzamal, H. (2022), "Study on the Mechanical Instability of Bidirectional Imperfect FG Sandwich Plates Subjected to In-Plane Loading", *Arab. J. Sci. Eng.*, **47**, 13655-13672. https://doi.org/10.1007/s13369-022-07203-8

Aghababaei, R. and Reddy, J.N. (2009), "Nonlocal third-order shear deformation plate theory with application to bending and vibration of plates", *J. Sound Vib.*, **326**(1-2), 277-289. https://doi.org/10.1016/j.jsv.2009.04.044.

Ahmed-Amine, D., Mohamed-Ouejdi, B., Drai, A., Mohamed, S. A.H., Mehmet, A., Tounsi, A., Mohamed, A.E. (2022), "Static analysis of functionally graded plate structures resting on variable elastic foundation under various boundary conditions", *Acta Mech*., 2022. https://doi.org/10.1007/s00707-022-03405-1

Akbaş, Ş.D. (2016), "Forced vibration analysis of viscoelastic nanobeams embedded in an elastic medium", *Smart Struct. Syst.*, **18**(6), 1125-1143. https://doi.org/10.12989/sss.2016.18.6.1125.

Akbaş, Ş.D. (2017), "Forced vibration analysis of functionally graded nanobeams", *Int. J. Appl. Mech.*, **9**(7), 1750100. https://doi.org/10.1142/S1758825117501009

Akbaş, Ş.D. (2018), "Forced vibration analysis of cracked nanobeams", *J. Brazilian Soc. Mech. Sci. Eng.*, **40**, 392. https://doi.org/10.1007/s40430-018-1315-1.

Baferani, A.H., Saidi, A.R. and Ehteshami, H. (2011) "Accurate solution for free vibration analysis of functionally graded thick rectangular plates resting on elastic foundation", *Compos. Struct.*, **93**(7), 1842-1853. https://doi.org/10.1016/j.compstruct.2011.01.020

Bui, V.T. (2022), "Free vibration behaviors of nanoplates resting on viscoelastic medium", *Ara. J. Scie. Eng.*, 2022. https://doi.org/10.1007/s13369-022-07500-2

Bui, V.T. and Gia, T.L. (2023), "Static Buckling Analysis of FG Sandwich Nanobeams", *J. Vib. Eng. Technol.*, 2023. https://doi.org/10.1007/s42417-023-01081-6

Cuong-Le, T., Khuong, D.N., Jaehong, L., Timon, R. and Hung, N.X. (2021), "A 3D nano scale IGA for free vibration and buckling analyses of multi-directional FGM nanoshells", *Nanot.*, **33**, 065703. https://doi.org/10.1088/1361-6528/ac32f9

Demir, C. and Oz, F.E. (2014), "Free vibration analysis of a functionally graded viscoelastic supported beam", *J. Vib. Control*, **20**(16), 2464-2486. https://doi.org/10.1177/1077546313479634.

Deng, Q., Kammoun, M., Erturk, A. and Sharma, P. (2014), "Nanoscale flexoelectric energy harvesting", *Int. J. Solids Struct.*, **51**(18), 3218-3225. https://doi.org/10.1016/j.ijsolstr.2014.05.018.

Doan, H.D, Do, V.T., Pham, H.C., Phung, V.M., Nguyen, X.N. (2022), "Vibration and static buckling behavior of variable

thickness flexoelectric nanoplates", *Mech. Bas. Des. Struct. Mach.*, **2022**, 1-19. https://doi.org/10.1080/15397734.2022.2088558.

Duc, H.D., Ashraf, M.Z. and Do, V.T. (2022), "Finite element modeling of free vibration of cracked nanoplates with flexoelectric effects", *The Euro. Phys. J. Plus.*, **137**, 447. https://doi.org/10.1140/epjp/s13360-022-02631-9

Duc, H. D., Thom, V. D., Phuc, M. P. and Nguyen, D. D. (2018a), "Validation simulation for free vibration and buckling of cracked Mindlin plates using phase-field method", *Mech. Adv. Mat. Struct.*, **26**(12), 1018-1027. https://doi.org/10.1080/15376494.2018.1430262

Duc, N. D., Trinh, T. D., Do, T. V. and Doan, D. H. (2018b), "On the buckling behavior of multi-cracked FGM plates", *Proc. Int. Conf. Adv. Comp. Mech.*, 29-45. https://doi.org/10.1007/978-981-10-7149-2_3

Ebrahimi, F., Karimiasl, M., Civalek, O., Vinyas, M. (2019a), "Surface effects on scale-dependent vibration behavior of flexoelectric sandwich nanobeams", *Adv. Nano. Res.*, **7**(2), 77-88. https://doi.org/10.12989/anr.2019.7.2.077

Ebrahimi, F., Barati, M.R. (2019b), "On static stability of electro-magnetically affected smart magneto-electro-elastic nano-plates", *Adv. Nano. Res.*, 63-75. https://doi.org/10.12989/anr.2019.7.1.063

Ebrahimi, F., Barati, M.R., Mahesh, V. (2019c), "Dynamic modeling of smart magneto-electro-elastic curved nanobeams", *Adv. Nano. Res.*, **7**(3), 145-155. https://doi.org/10.12989/anr.2019.7.3.145

Ebrahimi, F., Fardshad, R.E. and Mahesh, V. (2019d), "Frequency response analysis of curved embedded magneto-electro-viscoelastic functionally graded nanobeams", *Adv. Nano Res.*, **7**(6), 391-403. https://doi.org/10.12989/anr.2019.7.6.391.

Eichler, A., Moser, J., Chaste, J., Zdrojek, M., Wilson-Rae, I. and Bachtold, A. (2011), "Nonlinear damping in mechanical resonators made from carbon nanotubes and graphene", *Nat. Nanotechnol.*, **6**(6), 339-342. https://doi.org/10.1038/nnano.2011.71.

Foroutan, K. and Dai, L. (2022), "Post-buckling analysis of sandwich FG porous cylindrical shells with a viscoelastic core", *Steel Compose. Struct.*, **43**(3), 349-367. https://doi.org/10.12989/scs.2022.45.3.349.

Ghobadi, A., Golestanian, H., Beni, Y.T. and Żur, K.K. (2021), "On the size-dependent nonlinear thermo-electro-mechanical free vibration analysis of functionally graded flexoelectric nano-plate", *Commun. Nonlinear Sci. Numer. Simul.*, **95**, 105585. https://doi.org/10.1016/j.cnsns.2020.105585.

Hashemi, S.H., Mehrabani, H. and Ahmadi-Savadkoohi, A. (2015), "Exact solution for free vibration of coupled double viscoelastic graphene sheets by viscoPasternak medium", *Compos. Part B Eng.*, **78**, 377-383. https://doi.org/10.1016/j.compositesb.2015.04.008.

Hoang-Nam, N., Tran, C.T., Doan, T.L., Van-Duc, P., Do, V.T. and Phung, V.M. (2019a), "Research on the buckling behavior of functionally graded plates with stiffeners based on the third-order shear deformation theory", *Materials*, **12**(8), 1262. https://doi.org/10.3390/ma12081262.

Hoang-Nam, N., Tan-Y, N., Ke, V.T., Thanh, T.T., Truong-Thinh, N., Van-Duc, P. and Thom, V.D. (2019b), "A finite element model for dynamic analysis of triple-layer composite plates with layers connected by shear connectors subjected to moving load", *Materials*, **12**(4), 598. https://doi.org/10.3390/ma12040598

Hieu, N.T., Do, V.T., Thai, N.D., Long, T.D. and Minh, P.V. (2020), "Enhancing the quality of the characteristic transmittance curve in the infrared region of range 2.5-7 μ m of the optical magnesium fluoride (MgF2) ceramic using the hot-pressing technique in a vacuum environment", *Adv. Mater. Sci. Eng.*, **2020**. https://doi.org/10.1155/2020/7258431.

Jinxuan, Z., Zohre, M., Maryam, S. and Mohamed, A. K. (2022), "Intelligent modeling to investigate the stability of a two-dimensional functionally graded porosity-dependent nanobeam", *Comput. Concr.*, **30**(2), 85-97. https://doi.org/10.12989/cac.2022.30.2.085

Jing-Lei, Z., Wu, F., Ru-Qing, B. and Wang, S. (2022), "Guided waves of porous FG nanoplates with four edges clamped", *Adv. Nano. Res.*, **13**(5), 465-474. https://doi.org/10.12989/anr.2022.13.5.465

Karličić, D., Kozić, P. and Pavlović, R. (2014), "Free transverse vibration of nonlocal viscoelastic orthotropic multi-nanoplate system (MNPS) embedded in a viscoelastic medium", *Compos. Struct.*, **115** (1), 89-99. https://doi.org/10.1016/j.compstruct.2014.04.002.

Karličić, D., Cajić, M., Murmu, T. and Adhikari, S. (2015), "Nonlocal longitudinal vibration of viscoelastic coupled double-nanorod systems", *Eur. J. Mech. A Solids*, **49**, 183-196. https://doi.org/10.1016/j.euromechsol.2014.07.005.

Liang, X., Hu, S. and Shen, S. (2014), "Effects of surface and flexoelectricity on a piezoelectric nanobeam," *Smart Mater. Struct.*, **23** (3), 035020. https://doi.org/10.1088/0964-1726/23/3/035020.

Liang, X., Hu, S. and Shen, S. (2015), "Size-dependent buckling and vibration behaviors of piezoelectric nanostructures due to flexoelectricity", *Smart Mater. Struct.*, **24**(10), 105012. https://doi.org/10.1088/0964-1726/24/10/105012.

Liang, X., Yang, W., Hu, S. and Shen, S. (2016), "Buckling and vibration of flexoelectric nanofilms subjected to mechanical loads", *J. Phys. D. Appl. Phys.*, **49**(11), 115307. https://doi.org/10.1088/0022-3727/49/11/115307.

Li, A., Zhou, S. and Qi, L. (2016), "Size-dependent electro-mechanical coupling behaviors of circular micro-plate due to flexoelectricity", *Appl. Phys. A Mater. Sci. Proc.*, **122**, 918. https://doi.org/10.1007/s00339-016-0455-3.

Lieu, P.V. and Gia, T.L. (2023), "Static bending, free and forced vibration responses of organic nanobeams in a temperature environment", *Arch. Appl. Mech.*, 2023. https://doi.org/10.1007/s00419-023-02469-2

Luat, D.T, Do, V.T., Thanh, T.T., Minh, P.V, Ke, T.V, and Vinh, P.V. (2021), "Mechanical analysis of bi-functionally graded sandwich nanobeams", *Adv. Nano. Res.*, **11**(1), 55-71. https://doi.org/10.12989/anr.2021.11.1.055

Mahmoud, S.R., Ghandourah, E., Ali, A., Mohammed, B., Tounsi, A. and Fouad, B. (2022), "On thermo-mechanical bending response of porous functionally graded sandwich plates via a simple integral plate model", *Arch. Civil Mech. Eng.*, **22**, 186. https://doi.org/10.1007/s43452-022-00506-5

Majdoub, M.S., Sharma, P. and Cagin, T. (2008), "Enhanced size-dependent piezoelectricity and elasticity in nanostructures due to the flexoelectric effect", *Phys. Rev. B*, **77**, 119904. https://doi.org/10.1103/PhysRevB.77.125424.

Minh, T.T. and Thanh, C.L. (2022), "A nonlocal IGA numerical solution for free vibration and buckling analysis of porous sigmoid functionally graded (P-SFGM) nanoplate", *Int. J. Struct. Stab. Dyn.*, **22**(16), 2250193. https://doi.org/10.1142/S0219455422501930

Mohammadi, P., Liu, L.P. and Sharma, P. (2014), "A theory of flexoelectric membranes and effective properties of heterogeneous membranes", *J. Appl. Mech. Trans. ASME*, **81**(1), 011007. https://doi.org/10.1115/1.4023978.

Nam, V.H, Pham, V.V., Nguyen, V.C., Do, V.T. and Tran, T.H. (2019), "A new beam model for simulation of the mechanical behaviour of variable thickness functionally graded material beams based on modified first order shear deformation theory", *Materials*, **12**(3), 404. https://doi.org/10.3390/ma12030404

Nguyen, C.T., Nguyen, T.T. and Do, V.T. (2019), "New numerical

results from simulations of beams and space frame systems with a tuned mass damper", *Materials*, **12**(8), 1329. https://doi.org/10.3390/ma12081329

Pham, T.D., Doan, T.L. and Do, V.T. (2016), "Free vibration of functionally graded sandwich plates with stiffeners based on the third-order shear deformation theory", *Viet. J. Mech.*, **38**(2), 103-122. https://doi.org/10.15625/0866-7136/38/2/6730

Pham, H.C., Doan, H.D. and Do, V.T. (2022), "Phase field model for fracture based on modified couple stress", *Eng. Fract. Mech.*, **269**, 108534. https://doi.org/10.1016/j.engfracmech.2022.108534

Phung, M.V, Nguyen, D.T., Doan, L.T., Nguyen, D.V. and Duong, T.V. (2022), "Numerical investigation on static bending and free vibration responses of two-layer variable thickness plates with shear connectors", *Iran. J. Sci. Technol. Trans. Mech. Eng.*, **46**, 1047-1065. https://doi.org/10.1007/s40997-021-00459-9.

Phung, V.M., Le, M.T., Doan, T.L. and Nguyen, D.A.V. (2022), "Static bending analysis of nanoplates on discontinuous elastic foundation with flexoelectric effect". *J. Scie. Technol.*, **17**(5). https://doi.org/10.56651/lqdtu.jst.v17.n05.529

Pouresmaeeli, S., Ghavanloo, E. and Fazelzadeh, S.A. (2013), "Vibration analysis of viscoelastic orthotropic nanoplates resting on viscoelastic medium", *Compos. Struct.*, **96**, 405-410. https://doi.org/10.1016/j.compstruct.2012.08.051.

Qi, L., Zhou, S. and Li, A. (2016), "Size-dependent bending of an electro-elastic bilayer nanobeam due to flexoelectricity and strain gradient elastic effect", *Compos. Struct.*, **135**, 167-175. https://doi.org/10.1016/j.compstruct.2015.09.020.

Qi, L., Huang, S., Fu, G., Zhou, S. and Jiang, X. (2018), "On the mechanics of curved flexoelectric microbeams", *Int. J. Eng. Sci.*, **124**, 1-15. https://doi.org/10.1016/j.ijengsci.2017.11.022.

Quang, D.V., Doan T.N., Luat, D.T. and Thom, D.V. (2022), "Static analysis and boundary effect of FG-CNTRC cylindrical shells with various boundary conditions using quasi-3D shear and normal deformations theory", *Struct.*, **44**, 828-850. https://doi.org/10.1016/j.istruc.2022.08.039

Reissner, E. (1985), "Reflections on the theory of elastic plates", *Appl. Mech. Rev.*, **38**(11) 1453-1464. https://doi.org/10.1115/1.3143699

Rupa N.S. and Ray, M.C. (2017), "Analysis of flexoelectric response in nanobeams using nonlocal theory of elasticity", *Int. J. Mech. Mater. Des.*, **13**(3), 453-467. https://doi.org/10.1007/s10999-016-9347-0.

Shen, S. and Hu, S. (2010) , "A theory of flexoelectricity with surface effect for elastic dielectrics", *J. Mech. Phys. Solids*, **58**(5), 665-677. https://doi.org/10.1016/j.jmps.2010.03.001.

Singh, P.P., Azam, M.S. (2021), "Size dependent vibration of embedded functionally graded nanoplate in hygrothermal environment by Rayleigh-Ritz method", *Adv. Nano. Res.*, **10**(1), 25-42. https://doi.org/10.12989/anr.2021.10.1.025

Shu, L., Liang, R., Rao, Z., Fei, L., Ke, S. and Wang, Y. (2019), "Flexoelectric materials and their related applications: A focused review", *J. Adv. Ceram.*, **8**(2), 153-173. https://doi.org/10.1007/s40145-018-0311-3.

Shu, L., Wei, X., Pang, T., Yao, X. and Wang, C. (2011) , "Symmetry of flexoelectric coefficients in crystalline medium", *J. Appl. Phys.*, **110**, 104106. https://doi.org/10.1063/1.3662196.

Su, Y., Hao,W., Rungang, G., Zhi, Y., Jing, Z., Zhaohui, Z. and Yafei, Z. (2012), "Exceptional negative thermal expansion and viscoelastic properties of graphene oxide paper", *Carbon*, **50**(8), 2804-2809. https://doi.org/10.1016/j.carbon.2012.02.045.

Srivastava, I., Z. Yu, Z. and Koratkar, N. (2012), "Viscoelastic Properties of Graphene-Polymer Composites," *Adv. Sci. Eng. Med.*, **4** (1), 10-14. https://doi.org/10.1166/asem.2012.1127.

Tinh, Q.B., Duc, H.D., Thom, V.D., Sohichi, H. and Nguyen, D.D. (2016), "High frequency modes meshfree analysis of Reissner-Mindlin plates", *J. Sci. Adv. Mat. Develop.*, **1**(3), 400-412. https://doi.org/10.1016/j.jsamd.2016.08.005

Tien, D.M, Thom, D.V, Minh, P.V., Tho, N.C., Doan, T.N. and Mai, D.N. (2023), "The application of the nonlocal theory and various shear strain theories for bending and free vibration analysis of organic nanoplates", *Mech. Based Des. Struct.*, 2023. https://doi.org/10.1080/15397734.2023.2186893

Thai, L.M., Luat, D.T., Phung, V.B., Minh, P.V. and Thom, D.V. (2022), "Finite element modeling of mechanical behaviors of piezoelectric nanoplates with flexoelectric effects", *Arch. Appl. Mech.*, **92**(1), 163-182. https://doi.org/10.1007/s00419-021-02048-3.

Thanh, C. L., Khuong, D. N., Minh, H. L., Thanh, S. T., Phan-Vu, P. and Magd, A. W. (2022), "Nonlocal strain gradient IGA numerical solution for static bending, free vibration and buckling of sigmoid FG sandwich nanoplate", *Phys. B Cond. Mat.*, **631**, 413726. https://doi.org/10.1016/j.physb.2022.413726

Tho, N.C., Thom, D. Van, Cong, P.H., Zenkour, M.A., Doan, D.H. and Minh, P.V. (2023), "Finite element modeling of the bending and vibration behavior of three-layer composite plates with a crack in the core layer", *Compos. Struct.*, **305**, 116529. https://doi.org/10.1016/j.compstruct.2022.116529

Thom, V.D., Duc, H.D., Nguyen, D.D. and Tinh, Q.B. (2017), "Phase-field thermal buckling analysis for cracked functionally graded composite plates considering neutral surface", *Compos. Struct.*, **182**, 542-548. https://doi.org/10.1016/j.compstruct.2017.09.059

Thom, V.D., Duc, H.D., Nguyen, C.T. and Nguyen, D.D. (2022), "Thermal buckling analysis of cracked functionally graded plates", *Int. J. Struct. Stab. Dyn.*, **22**(8), 2250089. https://doi.org/10.1142/S0219455422500894.

Tho, N.C., Thanh, N.T., Tho, T.D., Minh, P.V. and Hoa, L.K. (2021), "Modelling of the flexoelectric effect on rotating nano-beams with geometrical imperfection", *J. Brazil. Soc. Mech. Sci. Eng.*, **43**(11), 510. https://doi.org/10.1007/s40430-021-03189-w.

Thom, D.V., Duc, D.H., Minh, P.V. and Tung, N.S. (2020), "Finite Element Modelling for Free Vibration Response of Cracked Stiffened Fgm Plates", *Vietnam J. Sci. Technol.*, **58**(1), 119. https://doi.org/10.15625/2525-2518/58/1/14278.

Tuan, L.T., Dung, N. T., Thom, D. V., Minh, P. V. and Zenkour, A. (2021), "Propagation of non-stationary kinematic disturbances from a spherical cavity in the pseudo-elastic cosserat medium", *Eur. Phys. J. Plus*, **136**, 1199. https://doi.org/10.1140/epjp/s13360-021-02191-4.

Tuyen, B.V. (2023), "Vibration response of bamboo-reinforced composite beams", *J. Vib. Eng. Technol.*, 2023. https://doi.org/10.1007/s42417-023-00998-2

Tran, N.D., Thom, D.V., Thanh, N.T., Chuong, P.V., Tho, N.C., Ta, N.T. and Nam, N.H. (2020), "Analysis of stress concentration phenomenon of cylinder laminated shells using higher-order shear deformation Quasi-3D theory", *Compos. Struct.*, **232**, 111526. https://doi.org/10.1016/j.compstruct.2019.111526.

Xiao, Z., Pinyi, W., Al-Dhaifallah, M., Muhyaddin, R. and Mohamed, A.K. (2022), "A machine learning-based model for the estimation of the critical thermo-electrical responses of the sandwich structure with magneto-electro-elastic face sheet", *Adv. Nano. Res.*, **12**(1), 81-99. https://doi.org/10.12989/anr.2022.12.1.081

Xiang, S. and Li, X.F. (2018), "Elasticity solution of the bending of beams with the flexoelectric and piezoelectric effects", *Smart Mater. Struct.*, **27**(10), 105023. https://doi.org/10.1088/1361-665X/aadd5b.

Xiang, S., Lee, K.Y. and Li, X.F. (2020), "Elasticity solution of functionally graded beams with consideration of the flexoelectric effect", *J. Phys. D. Appl. Phys.*, **53**(10), 105301. https://doi.org/10.1088/1361-6463/ab5cc1.

Yan, Z. and Jiang, L.Y. (2013a), "Flexoelectric effect on the electroelastic responses of bending piezoelectric nanobeams", *J. Appl. Phys.*, **113**(19), 194102. https://doi.org/10.1063/1.4804949.

Yan, Z. and Jiang, L. (2013b), "Size-dependent bending and vibration behaviour of piezoelectric nanobeams due to flexoelectricity", *J. Phys. D. Appl. Phys.*, **46**(35), 355502. https://doi.org/10.1088/0022-3727/46/35/355502.

Yang, W., Liang, X. and Shen, S. (2015), "Electromechanical responses of piezoelectric nanoplates with flexoelectricity", *Acta Mech.*, **226**(9), 3097-3110. https://doi.org/10.1007/s00707-015-1373-8.

Yue, Y.M., Xu, K.Y. and Chen, T. (2016), "A micro scale Timoshenko beam model for piezoelectricity with flexo-electricity and surface effects", *Compos. Struct.*, **136**, 278-286. https://doi.org/10.1016/j.compstruct.2015.09.046.

Zenkour, A.M. (2016), "Nonlocal transient thermal analysis of a single-layered graphene sheet embedded in viscoelastic medium", *Physica. E*, **79**, 87-97. https://doi.org/10.1016/j.physe.2015.12.003.

Zhang, Z., Yan, Z. and Jiang, L. (2014), "Flexoelectric effect on the electroelastic responses and vibrational behaviors of a piezoelectric nanoplate", *J. Appl. Phys.*, **116**, 014307. https://doi.org/10.1063/1.4886315.

Zhang, Z. and, Jin, C. (2022), "Axisymmetric vibration analysis of a sandwich porous plate in thermal environment rested on Kerr foundation", *Steel Compos. Struct.*, **43**(5), 581-601. https://doi.org/10.12989/scs.2022.43.5.581

Zhou, L. (2022), "Computerized responses of spinning NEMS via numerical and mathematical modeling", *Struct. Eng. Mech.*, **82**(5), 629-641. https://doi.org/10.12989/sem.2022.82.5.629.

Zhonghong, L. and Gongxing, Y. (2022), "Machine learning for structural stability: Predicting dynamics responses using physics-informed neural networks", *Compit. Concr.*, **29**(6), 419-432. https://doi.org/10.12989/cac.2022.29.6.419

Zubko, P., Catalan, G. and Tagantsev, A.K. (2013) "Flexoelectric effect in solids", *Annual Rev. Mater. Res.*, **43**, 387-421. https://doi.org/10.1146/annurev-matsci-071312-121634.

Wang, Y., Li, F.M. and Wang, Y.Z. (2015), "Nonlinear vibration of double layered viscoelastic nanoplates based on nonlocal theory", *Physiaca E*, **67**, 65-76. https://doi.org/10.1016/j.physe.2014.11.007.

Wang, X., Zhang, R. and Jiang, L. (2017), "A study of the flexoelectric effect on the electroelastic fields of a cantilevered piezoelectric nanoplate", *Int. J. Appl. Mech.*, **9**(4), 1750056. https://doi.org/10.1142/S1758825117500569.

Wang, K.F. and Wang, B.L. (2018), "Energy gathering performance of micro/nanoscale circular energy harvesters based on flexoelectric effect", *Energy*, **149**, 597-606. https://doi.org/10.1016/j.energy.2018.02.069.

Wenjuan Y. (2022), "Intelligent computer modelling and simulation for the large amplitude of nano systems", *Adv. Nano Res.*, **13**(1), 63-75. https://doi.org/10.12989/anr.2022.13.1.063

Zhe, Z., Qijian, Y. and Cong, J. (2022), "Axisymmetric vibration analysis of a sandwich porous plate in thermal environment rested on Kerr foundation", *Steel Compos. Struct.*, **43**(5), 581-601. https://doi.org/10.12989/scs.2022.43.5.581

Smain, B., Aicha, B., Mohammed, S. A. H. and Marc, A. (2022), "A new quasi-3D plate theory for free vibration analysis of advanced composite nanoplates", *Steel Compos. Struct.*, **45**(6), 839-850. https://doi.org/10.12989/scs.2022.45.6.839

Lingao, Z. (2022), "Computerized responses of spinning NEMS via numerical and mathematical modeling", *Struct. Eng. Mech.*, **82**(5), 629-641. https://doi.org/10.12989/sem.2022.82.5.629

Zhonghong, L. and Gongxing, Y. (2022), "Machine learning for structural stability: Predicting dynamics responses using physics-informed neural networks", *Comput. Concr.*, **29**(6), 419-432. https://doi.org/10.12989/cac.2022.29.6.419

Jinxuan, Z., Zohre, M., Maryam, S. and Mohamed, A.K. (2022), "Intelligent modeling to investigate the stability of a two-dimensional functionally graded porosity-dependent nanobeam", *Comput. Concr.*, **30**(2), 85-97. https://doi.org/10.12989/cac.2022.30.2.085

Xiao, Z., Pinyi, W., Al-Dhaifallah, M., Muhyaddin, R. and Mohamed, A.K. (2022), "A machine learning-based model for the estimation of the critical thermo-electrical responses of the sandwich structure with magneto-electro-elastic face sheet", *Adv. Nano. Res.*, **12**(1), 81-99. https://doi.org/10.12989/anr.2022.12.1.081

Jing-Lei, Z., Gui-Lin, S., Fei, W., Shu-Jin, Y., Ru-Qing, B., Hua-Yan, P., Shilong, W., Jun, L. (2022), "Guided waves of porous FG nanoplates with four edges clamped", *Adv. Nano. Res.*, **13**(5), 465-474. https://doi.org/10.12989/anr.2022.13.5.465

CC